Journal of Molecular Graphics and Modelling 39 (2013) 118–125

Contents lists available at SciVerse ScienceDirect

Journal of Molecular Graphics and Modelling

journal homepage: www.elsevier.com/locate/JMGM

# Parameterization of the proline analogue Aze (azetidine-2-carboxylic acid) for molecular dynamics simulations and evaluation of its effect on homo-pentapeptide conformations

Kyrylo Bessonov [1], Kenrick A. Vassall, George Harauz *

*Department of Molecular and Cellular Biology, University of Guelph, 50 Stone Road East, Guelph, Ontario N1G 2W1, Canada*

ARTICLE INFO

*Article history:*
Received 18 July 2012
Received in revised form 11 October 2012
Accepted 17 November 2012
Available online 29 November 2012

*Keywords:*
Aze (azetidine-2-carboxylic acid)
Poly-proline II
*cis–trans* Isomerization
Molecular dynamics
GROMACS: myelin basic protein
Intrinsically disordered protein
Multiple sclerosis

ABSTRACT

We have parameterized and evaluated the proline homologue Aze (azetidine-2-carboxylic acid) for the gromos56a3 force-field for use in molecular dynamics simulations using GROMACS. Using bi-phasic cyclohexane/water simulation systems and homo-pentapeptides, we measured the Aze solute interaction potential energies, ability to hydrogen bond with water, and overall compaction, for comparison to Pro, Gly, and Lys. Compared to Pro, Aze has a slightly higher H-bonding potential, and stronger electrostatic but weaker non-electrostatic interactions with water. The 20-ns simulations revealed the preferential positioning of Aze and Pro at the interface of the water and cyclohexane layers, with Aze spending more time in the aqueous layer. We also demonstrated through simulations of the homo-pentapeptides that Aze has a greater propensity than Pro to undergo *trans*→*cis* peptide bond isomerization, which results in a severe 180° bend in the polypeptide chain. The results provide evidence for the hypothesis that the mis-incorporation of Aze within proline-rich regions of proteins could disrupt the formation of poly-proline type II structures and compromise events such as recognition and binding by SH3-domains.



## 1. Introduction

The non-protein imino acid azetidine-2-carboxylic acid (Aze, also denoted AZC in the literature) is similar to proline (2-carboxypyrrolidine, Pro), except that it has a 4-atom instead of a 5-atom ring (Fig. 1) [1,2]. This unusual imino acid was first discovered to occur naturally in plants of the *Liliaceae* family, specifically lily-of-the-valley (*Convallaria majalis*) [3]. It has since been found to occur naturally in many other plants, such as sugar beets (*Beta vulgaris*, formerly of *Chenopodiaceae*, now of *Amaranthaceae*) [4–7] and garden beets [8]. These "non-protein amino/imino acids" are important to plants in metabolic processes and as a defense mechanism [6,7,9,10].

When Aze is added endogenously to the media of cultured eukaryotic cells, it is recognized by the Pro-tRNA and is readily incorporated into proteins such as collagen, keratin, haemoglobin, and calnexin [8,11–18]. The homologue has also been shown to affect cell growth and proline metabolism when added to *E. coli*, both wild-type and proline auxotrophs [19–21]. We have recently shown that it could be mis-incorporated into *E. coli* expressing recombinant proteins such as myelin basic protein (MBP), but the viability of the cultures is decreased [22]. Some organisms such as yeast detoxify the compound by expressing *N*-acetyltransferases [23–25]. Other cells invoke a heat-shock response due to protein mis-folding [26–30].

The diverse toxic effects of Aze on animals are summarized by Rubenstein [31]. One example is the observation of severe neurodegeneration in sheep, including pregnant ewes that are fed a diet rich in beet by-products [32], and we note some other particular examples [33–35]. Rubenstein has further hypothesized that the misincorporation of Aze into proteins during brain development may contribute to inherently unstable myelin, which may be one of many factors predisposing an individual to developing multiple sclerosis (MS) [36,37]. Significantly, Aze enters the human food chain indirectly, since "beet molasses" from sugar production is used in many areas to feed cattle [17]. At present, the worldwide distribution of MS correlates with high rates of sugar beet production, *e.g.*, in the province of Alberta which has one of the highest rates of MS in Canada [38]. This hypothesis falls within the rubric of an "inside-out" model, which suggests that MS is caused by a cytodegenerative process aimed at the oligodendrocyte–myelin

*Abbreviations:* Aze, azetidine-2-carboxylic acid; MBP, myelin basic protein; GROMACS, GROningen MAchine for Chemical Simulations; MD, molecular dynamics; MS, multiple sclerosis; PDB, Protein Data Bank; PPI, poly-proline type I conformation; PPII, poly-proline type II conformation; SH3, Src homology 3.

* Corresponding author. Tel.: +1 519 824 4120x52535.
*E-mail address:* gharauz@uoguelph.ca (G. Harauz).
[1] Present address: Department of Electrical Engineering and Computer Science (Institut Montefiore), University of Liège, 4000 Liège 1, Belgium.

1093-3263/$ – see front matter © 2012 Elsevier Inc. All rights reserved.
http://dx.doi.org/10.1016/j.jmgm.2012.11.006

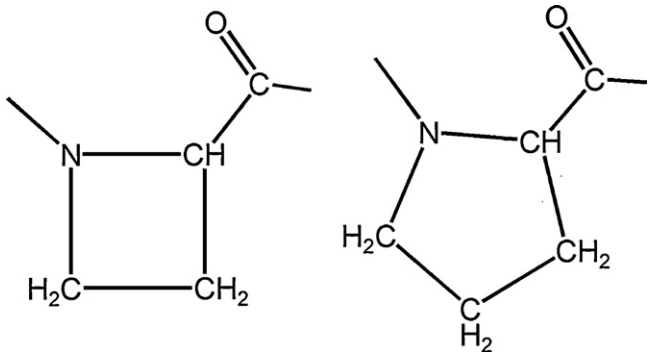


**Fig. 1.** Molecular structures of Aze (left) and Pro (right).

complex [39–41]. Gradual demyelination can then lead to an autoimmune response and a cycle of further degeneration, characteristic of the most common relapsing-remitting manifestation of MS.

Since the cause of MS remains unknown over 150 years since its first major clinical documentation [42], Rubenstein's hypothesis bears closer examination, including demonstrating the effects of Pro-to-Aze substitution in essential myelin proteins such as MBP [43–47]. This protein is multifunctional within myelin, acting both to adhere membrane leaflets together, and as a hub in protein–protein and protein–membrane interaction networks (actin and tubulin cytoskeleton, SH3-domain containing proteins, and calcium-activated calmodulin) [48–51]. We have determined that a central proline-rich region is functionally significant [46,50,52–56], and by molecular dynamics (MD) simulations have demonstrated that phosphorylation at key kinase targets affects its conformation, particularly a poly-proline (PPII) structure formed here [55]. We have recently conjectured that Pro-to-Aze mis-incorporation would have severe effects on the protein at the molecular level [22], particularly its interaction with SH3-domain-containing proteins [50–53,55,56]. Because of the difficulty, expense, and hazard of producing recombinant Aze-containing MBP for experimental investigations, it is worthwhile to pursue MD simulations. Towards this end, we present here a full parameterization of Aze for future MD studies using GROMACS [57,58], and illustrate its effects on the conformations of some simple homo-pentapeptides, in preparation for studies on larger protein segments. Since GROMOS force-fields are primarily used for protein simulations, accurate estimation of parameters for amino acids is crucial [59].

## 2. Methods

### 2.1. Parameterization of Aze topology in the GROMACS gromos53a6 force-field

Force-fields are essential components of any MD simulations, as they describe the simulation environment by assigning physical constants and empirical charges to all chemical species contained in a particular system. In the case of the GROMOS force-fields, most of the parameters are empirically determined, which makes parameterization of new chemical species, particularly the accurate estimation of atomic partial charges, a laborious task. Here, we decided to use a semi-automatic approach to parameterize Aze accurately. The structure of Aze was derived from that of Pro by elimination of the $CH_2$ group from the aliphatic ring, which facilitated the validation process (Fig. 1). The PRODRG2 online server [60] in conjunction with the Pro reference parameters was used to derive the Aze parameters for bonds, dihedral angles, improper dihedral and other angles, as discussed in detail in the Supplementary Information.

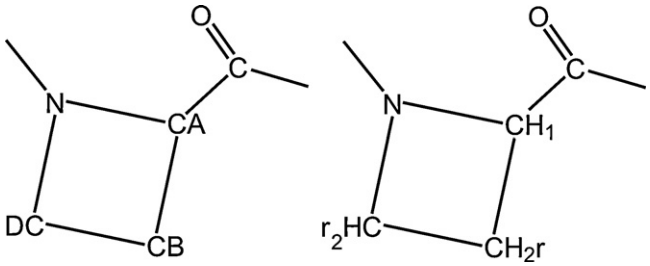


**Fig. 2.** Representations of Aze using the default Protein Data Bank (left) and gromos56a3 (right) nomenclatures. Please refer to Fig. S1 for the detailed Aze topology interpretation in the context of the gromos56a3 force-field.

Improper and proper dihedral angles of the Aze topology were almost identical to those of Pro, due to structural similarity. The only small modification was defined by the <(CA CB CD N) and <(N CA CB CD) angles, part of the 4-membered ring defined under gromos53a6 dihedral torsion type angles 34 (gd_34) (Fig. 2 and Fig. S1).

### 2.2. Validation of Aze parameters by QM calculations

The partial charges predicted by the PRODRG server were checked by *ab initio* QM calculations since accurate derivation of partial charges is essential, as discussed in Ref. [61]. The Hartree–Fock *ab initio* model with the 6-311G basis set of wave functions describing the atomic orbitals was used in all QM calculations. The final calculation of partial charges also employed an electro-static potential (ESP) fitting that considers interaction energies [62]. The overall charge of zero and electron spin multiplicity of one were specified for both the Aze and Pro residues. The QM calculations were performed on a single residue with uncharged termini, to represent more closely the context of the residue being part of a polypeptide chain (Fig. S2). The QM runs were done both for Pro and Aze, for comparison purposes. The charges assigned by Gromos53a6 were taken as a reference. The Gaussian 09 software package was used for all QM calculations [http://www.gaussian.com/g_tech/g_ur/m_citation.htm; Gaussian, Inc., Wallingford, CT].

### 2.3. Molecular dynamics simulations of Aze-containing peptides

The evaluation of the behaviour of Aze within GROMACS was performed by molecular dynamics simulations of homo-pentapeptides in aqueous and mixed solvent (cyclohexane/water) systems. Molecular dynamics simulations were performed using the GROMACS 4.5.5 software package [57,58] and the Gromos96 ffG53a6 force-field [59], at 310 K and 1 bar for total of 20 ns. Molecular dynamics production runs were performed using 64 processors at the Compute Canada/SharcNet facilities (https://www.sharcnet.ca). For visualization and analysis of structural files and trajectories computed by GROMACS, the GROMACS utilities and the Visual Molecular Dynamics (VMD) program [63] were utilized. The custom scripts for VMD were written in the TCL language to compute the $\varphi$, $\psi$, and $\omega$ dihedral angles. The frequency of conversion of the peptide bond from *cis* to *trans* conformation as well as the duration of time spent in each conformation was evaluated using custom Perl scripts.

### 2.4. Evaluation of the Aze topology parameters using bi-phasic and pure aqueous systems

The derived Aze topology parameters were evaluated in bi-phasic interfacial systems consisting of non-polar cyclohexane and polar spc216 water solvents. Such systems allow visualization of

the behaviour of the simulated molecule in both hydrophobic and hydrophilic environments.

The topology of cyclohexane (*.itp) was obtained from a previous study [61] that used the PRODRG2 server to derive it. All simulated systems followed the same method by first positioning the peptide at the interface of both solvents (*i.e.*, the centre of the simulation box). The density of the cyclohexane solvent was consistent with the experimental value of 0.779 g/L. The final dimensions of the simulated box were 3 nm × 3 nm × 4 nm with 2250 atoms. Four systems were assembled containing 5-residue homo-peptides made up either of Aze, Pro, Gly, or Lys, respectively. Systems were simulated at 37 °C and an initial reference pressure of 1 atm, for a total of 20 ns.

A purely aqueous environment was also evaluated. The homo-pentapeptides of Aze, Pro, Gly, and Lys were solvated with spc216 water molecules in 3 nm × 3 nm × 4 nm boxes to an overall density of 0.99 g/L. The pure water systems were simulated at 37 °C and 1 atm initial pressure, for a total of 20 ns.

### 2.5. The trans-to-cis isomerization potential of the Aze peptide bonds

The overall propensity of Aze to induce *trans*↔*cis* transitions was compared to that of Pro. The isomerization potential of the Aze residue to promote *cis* peptide bonds was investigated by measuring peptide bond omega angles ($\omega$) along the whole trajectory of 20 ns. The results were compared across simulated systems.

The following MD protocol was used to induce isomerization of the peptide bond. The energy-minimized water boxes containing either Aze or Pro homo-pentapeptides were re-simulated using new simulation conditions. The simulation temperature was set to 800 °C throughout the simulation in order to observe isomerization events within the ns scale. The constraints were only enabled with regards to bond lengths. Two simulation groups (peptide and water) were separately thermally coupled. The initial reference pressure was simulated using the isotropic Berendsen barostat at 1 bar.

## 3. Results and discussion

### 3.1. The QM estimation of charges confirms correct assignment of partial charges

The accuracy of the derived Aze topology is essential to assess, since partial charges play a major role on how the newly derived molecule behaves in MD simulations [61]. Thus, we cross-validated the accuracy of the neutral charge assignment to the Aze ring carbons (*i.e.*, CD and CB) using the *ab initio* Hartree–Fock (HF) method using a 6-311G basis set (Table 1). Since gromos53a6 is a united atom force-field, the aliphatic hydrogens are not considered during MD calculations and, thus, the sum of charges of the $CH_2$ group represents the partial charges of the carbon atoms according to this force-field.

The resultant point charges (*e*) for those carbons both in Pro and Aze were very close to the neutral values of the gromos53a6 force-field (Table 1 and Fig. S2). As a reference for our QM method of calculating partial charges, we had used a reference structure of Pro, whose partial charges are known accurately, also obtaining close to neutral partial charges for the ring $CH_2$ groups (Table 1). Our QM results justify the assignment of a neutral charge to the 4-membered ring carbons during Aze topology derivation.

To ensure that the 420 kJ/mol force constant of the Aze ring angles <(CA N CD), <(N CA CB), <(CA CB CD), <(N CD CB) is valid, the right angle fluctuation was monitored over the course of the simulation. The fluctuation over the course of the whole simulation was only 2.5°, highlighting the rigidity and stability of the structure under the assigned constant.

**Table 1**
Partial charges of Aze and Pro calculated *via* an *ab initio* Hartree–Fock (HF) method.

| Molecule | Group | Atom name | Partial charges (*e*) | | |
|---|---|---|---|---|---|
| | | | Element | Hartree–Fock | gromos53a6 |
| Pro | $NH_2$ | N | N | −0.246 | 0 |
| | | H1 | H | 0.294 | NA |
| | | H2 | H | 0.406 | NA |
| | | Sum | | 0.454 | 0 |
| | CH | CA | C | 0.323 | 0 |
| | | HA | H | 0.01 | NA |
| | | Sum | | 0.333 | 0 |
| | CHO | C | C | 0.939 | 0.45 |
| | | O | O | −0.841 | −0.45 |
| | | HC | H | 0.102 | NA |
| | | Sum | | 0.2 | 0 |
| | $CH_2$ | CB | C | −0.334 | 0 |
| | | HB1 | H | 0.098 | NA |
| | | HB2 | H | 0.067 | NA |
| | | Sum | | −0.169 | 0 |
| | $CH_2$ | CD | C | −0.018 | 0 |
| | | HD1 | H | 0.042 | NA |
| | | HD2 | H | 0.051 | NA |
| | | Sum | | 0.075 | 0 |
| | $CH_2$ | CG | C | 0.162 | 0 |
| | | HG1 | H | −0.009 | NA |
| | | HG2 | H | −0.003 | NA |
| | | Sum | | 0.15 | 0 |
| Aze | $NH_2$ | N | N | −0.109 | 0 |
| | | H1 | H | 0.254 | NA |
| | | H2 | H | 0.252 | NA |
| | | Sum | | 0.397 | 0 |
| | CH | CA | C | 0.164 | 0 |
| | | HA | H | 0.036 | NA |
| | | Sum | | 0.2 | 0 |
| | CHO | C | C | −0.322 | 0.45 |
| | | O | O | −0.663 | −0.45 |
| | | HC | H | 0.175 | NA |
| | | Sum | | −0.81 | 0 |
| | $CH_2$ | CB | C | 0.038 | 0 |
| | | HB1 | H | 0.089 | NA |
| | | HB2 | H | 0.004 | NA |
| | | Sum | | 0.131 | 0 |
| | $CH_2$ | CD | C | −0.174 | 0 |
| | | HD1 | H | 0.123 | NA |
| | | HD2 | H | 0.103 | NA |
| | | Sum | | 0.052 | 0 |

*Note*: Since gromos53a6 is a united atom force-field, the aliphatic hydrogens are omitted and are represented by "not applicable" (NA) designations. The atom names follow the PDB nomenclature (Fig. 2).

### 3.2. Properties of Aze in aqueous and binary systems

Further evaluation of Aze behaviour was performed and compared to other simulated residues by molecular dynamics simulations of homo-pentapeptides in aqueous and mixed solvent systems, measuring key parameters such as overall position of the peptide, overall structure compaction, H-bonding potential, and interaction strength with the solvent. In Fig. 4, we show the final snapshots of the trajectories of all four simulated homo-pentapeptides: Aze, Pro, Gly, and Lys. The Aze, Pro, and Gly homo-pentapeptides are positioned at the interface between the layers, which provides an amphipathic environment that will be preferred by residues with zero net charge. The similar behaviour and stability of Aze compared to Pro in this interfacial system is expected given that that these two imino acids have comparable structure, partial atomic charges and bond force constants. Finally, the positively charged Lys partitioned preferentially, into the polar aqueous environment (Fig. 4).

**Table 2**
Homo-pentapeptide solvent interaction measurements in water/cyclohexane bi-phasic systems using the gromos53a6 force-field.

| Measurement | AZE | PRO | GLY | LYS |
|---|---|---|---|---|
| Average Radius of Gyration $R_g$ (nm) | 0.503 | 0.510 | 0.450 | 0.610 |
| Average # of H-bonds per 100 ps | 4.975 | 4.229 | 9.516 | 19.195 |
| Coulombic–Short Range ($F_{elect}$): Protein–non-Protein (kJ/mol) | −142.181 | −121.867 | −254.724 | −887.974 |
| LJ-Short Range ($F_{vdv}$): Protein–non-Protein (kJ/mol) | −126.497 | −157.708 | −61.515 | −12.771 |

Further assessment of the Aze parameterization quality was done by estimating the homo-pentapeptide non-bonding (Coulombic and Lennard–Jones) energies and hydrogen bonding potential with water using both bi-phasic (Table 2) and water only (Table 3) systems. The results were compared to Pro, Gly, and Lys.

The average number of H-bonds averaged over the whole trajectory varied amongst the residues with a rank order of Lys > Gly > Aze > Pro (Tables 2 and 3). As expected, Lys, which has a positively charged side chain, forms the most hydrogen bonds. The H-bonding behaviours of Aze and Pro were the most comparable amongst the investigated residues, and both were lower than Gly, despite the latter having similar net charge. This result suggests that the cyclic ring structures of Aze and Pro prevent H-bonding with solvent molecules compared to the more extended amino acids. The finding that the hydrogen-bonding potential of Aze is slightly higher than that of Pro could be due to the slightly smaller size of Aze, which may allow for more solvent molecules to cluster around it.

We also investigated the Aze electrostatic interaction potential *via* Coulombic short-range forces ($F_{elect}$) between peptide and solvent. Again, Aze was shown to have a comparable but stronger electrostatic potential compared to Pro (Tables 2 and 3). Interestingly, the differences between attractive Coulombic forces, $F_{elect}$, between Aze and Pro were more pronounced in the bi-phasic systems (−20.3 kJ/mol), compared to completely aqueous systems (−8.6 kJ/mol). Analysis of trajectory files revealed that Pro spent more time in the hydrophobic cyclohexane phase compared to Aze, reducing the Pro electrostatic forces that could only have been generated in the aqueous phase, and not in non-polar cyclohexane (data not shown). As expected from the positively charged control, Lys showed the greatest overall favourable electrostatic attraction force (Tables 2 and 3).

Finally, we evaluated the van der Waals non-electrostatic interactions ($F_{vdv}$) occurring between non-charged atoms (*e.g.*, cyclohexane). This type of interaction is highly pronounced in non-polar systems. The Aze showed a weaker van der Waals interaction potential compared to Pro in both systems, which could be explained by the bulkier 5-membered ring of Pro, compared to the smaller 4-membered ring of Aze. Conversely, Lys had the largest value amongst Aze, Pro, and Gly, suggesting that non-electrostatic forces ($F_{vdv}$) are minor compared to the effect of electrostatic forces ($F_{elect}$) during solvent interaction.

### 3.3. Isomerization potential of the Aze residue

Peptide bond isomerization is a crucial process that is characterized by considerable structural disruption and changes in ligand-binding specificities. For example, secondary structure transitions of a poly-proline type II to type I conformation (PPII *versus* PPI, respectively) occur through *trans* to *cis* isomerization, and are a naturally occurring process that occurs in intra-molecular switches, *e.g.*, upon SH3-domain containing ligand binding [46,64–66]. Peptide bond isomerization is a slow naturally occurring process on the seconds scale, requiring a significant energy input of ∼50–100 kJ/mol, depending on the residue, and, *trans*→*cis* is less energetically favourable than *cis*→*trans* [67]. Peptidyl-prolyl isomerases are known to facilitate peptide bond transitions *in vivo* [68–70]. Here, we examined the propensity of Aze to undergo such transitions, to understand further structural fluctuations in key motifs such as PPII in proline-rich segments of proteins such as MBP [50–53,56], and possible mechanisms of toxicity of this residue [17,36].

It is challenging to study spontaneous peptide bond isomerization *in silico*, as currently MD simulations are in the millisecond range, in spite of promising applications of graphics processing units (GPUs) in scientific computing and molecular dynamics packages such as GROMACS 4.5.5 [71]. In addition, the molecular mechanisms mediating isomerization might be of a complex nature requiring a significant energy input, and more in-depth QM/MD simulations. Here, none of the 20-ns simulations of the Aze, Pro, Gly, and Lys homo-pentapeptides in water at 37 °C, with an initial *trans* conformation of all peptide bonds, showed *trans*→*cis* shifts, as ascertained by the $\omega$ angle calculation for each trajectory. A longer simulation of 200 ns also did not show any isomerization for Aze; nor did simulations at 72 °C and 200 °C. Using experimental data, the empirically determined rate constant allowed us to estimate the temperature required to see isomerization events at the ns scale (p. 170 in [72]). Here, a temperature of 800 °C was selected for 20-ns simulations in water, that finally yielded significant numbers of *trans*→*cis* and *cis*→*trans* isomerization events to evaluate.

The overall propensity of Aze compared to Pro to undergo *trans*→*cis* and *cis*→*trans* transitions of the peptide bond was measured by counting the frequency of the peptide bonds to undergo both transitions (isomerizations). The frequency was summarized by the probability of [CIS] and [TRANS] states expressed as $p_{cis}$ and $p_{trans}$ (Fig. 5). Since the Aze isomerization potential could be influenced by the context of the whole protein, where flexibility of the peptide bond might be affected by other factors such as intra- and inter-residue interactions, we also considered the inner peptide bond angles located at residues 2, 3, and 4 ($\omega_2$ and $\omega_3$) (Fig. 3). On average, the probability of finding the peptide bond in the *cis* conformation (the [CIS] state) is twice as high in the Aze homo-pentapeptide as compared to the Pro homo-pentapeptide (Fig. 5), regardless whether considering all ($\omega_1$, $\omega_2$, $\omega_3$, $\omega_4$) or only inner angles ($\omega_2$, $\omega_3$). This result was confirmed by 5 independent simulations, run under identical conditions, over 20 ns.

To demonstrate that the difference in [CIS] state frequency between the Aze and Pro homo-pentapeptides is statistically significant, we performed a two sample unpaired *t*-test at $\alpha = 0.05$

**Table 3**
Homo-pentapeptide solvent interaction measurements in pure water systems using the gromos53a6 force-field.

| Measurement | AZE | PRO | GLY | LYS |
|---|---|---|---|---|
| Average Radius of Gyration $R_g$ (nm) | 0.499 | 0.503 | 0.441 | 0.607 |
| Average # of H-bonds per 100 ps | 7.212 | 7.069 | 12.304 | 23.106 |
| Coulombic-Short Range ($F_{elect}$): Protein–non-Protein (kJ/mol) | −187.303 | −178.670 | −312.337 | −949.128 |
| LJ-Short Range ($F_{vdv}$): Protein–non-Protein (kJ/mol) | −109.648 | −134.341 | −46.137 | −0.222 |

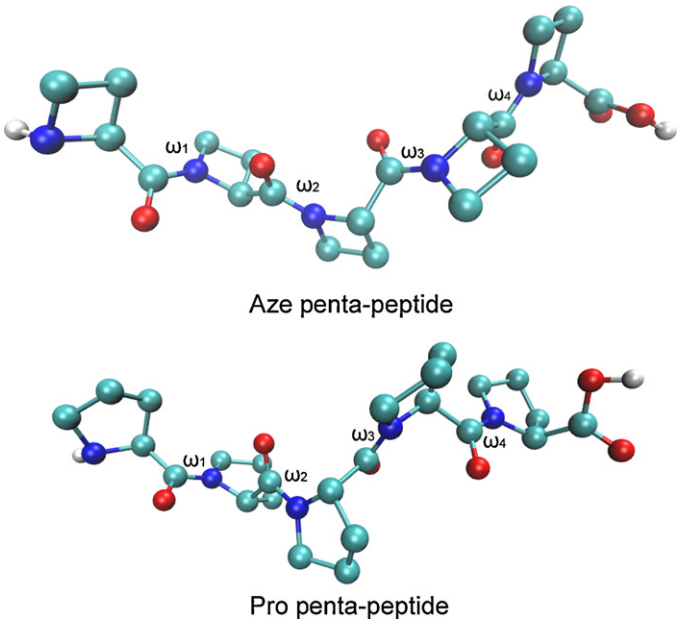


**Fig. 3.** Homo-pentapeptides of Aze and Pro in *trans* peptide bond conformation with omega angles ($\omega_1$ to $\omega_4$) shown.

($p < 0.05$ are significant), obtaining $p$-values of only $1.61 \times 10^{-4}$ (if only considering $\omega_1$, $\omega_2$, $\omega_3$, $\omega_4$) and $3.90 \times 10^{-4}$ (if only considering $\omega_2$, $\omega_3$). This result allowed us to accept the alternative $t$-test hypothesis ($H_a$) stating that the *cis* conformation in the Aze homo-pentapeptide had a significantly higher probability of occurrence than in the Pro homo-pentapeptide (Fig. 5). Interestingly, the peptide bond between the central residues (2,3 and 3,4, *i.e.*, $\omega_2$ and $\omega_3$, respectively) in the *cis* conformation ([CIS] state) occurred 1.15 times less frequently compared to those at the N- and C-terminal residues (1,2 and 4,5, *i.e.*, $\omega_1$ and $\omega_4$), respectively, as shown by lower $p_{cis}$ values. This result is possibly due to adjacent residues on either end hindering their mobility (data not shown), and implies that the value of $p_{cis}$ will depend on a multitude of factors (*e.g.*, H-bonding, electrostatic interactions, steric effects) in a given protein structure. In addition, $p_{cis} < 0.5$ in all instances indicates that the [TRANS] state is favoured over the [CIS] state.

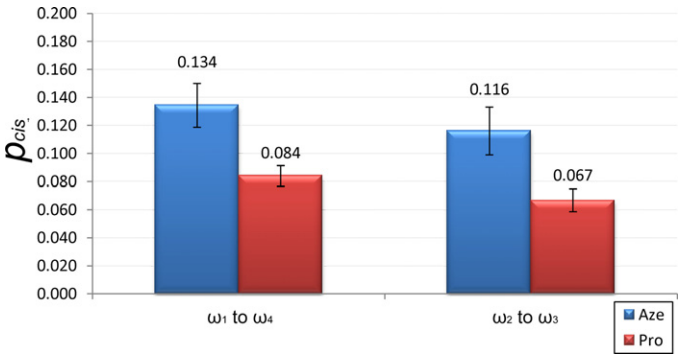


**Fig. 5.** Overall probability of the peptide bond to be found in the *cis* conformation (*i.e.*, the [CIS] state) measured throughout 20-ns simulations of homo-pentapeptide Aze and of homo-pentapeptide Pro in $H_2O$, repeated 5 times. The *cis* state probability ($p_{cis}$) measured for both $\omega_1$ to $\omega_4$, and $\omega_2$ to $\omega_3$, of the corresponding homo-pentapeptides. The error bars represent standard deviations.

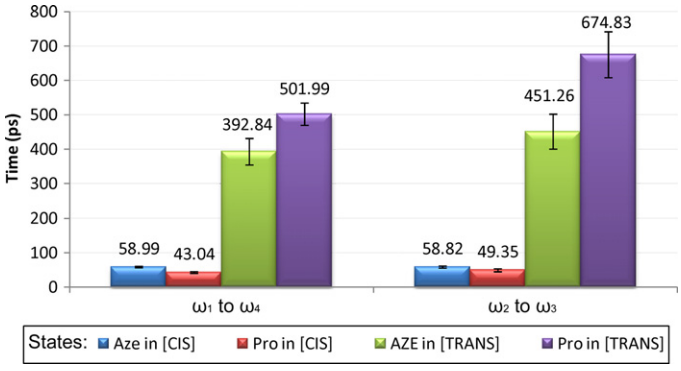


**Fig. 6.** Mean duration of [CIS] and [TRANS] states for $\omega_1$ to $\omega_4$ (all angles), and for $\omega_2$ to $\omega_3$ (inner angles), in the Aze and Pro homo-pentapeptides simulated for 20 ns in $H_2O$ at 800 °C, repeated 5 times. The error bars represent standard deviations.

Whereas these results provided evidence that, on average, Aze more strongly induces a *cis* peptide bond conformation, they did not highlight the duration of the [CIS] state in Aze and Pro homo-pentapeptides. Again, we considered both the $\omega_1$ to $\omega_4$, and the $\omega_2$ to $\omega_3$ cases, to represent both average and protein structure

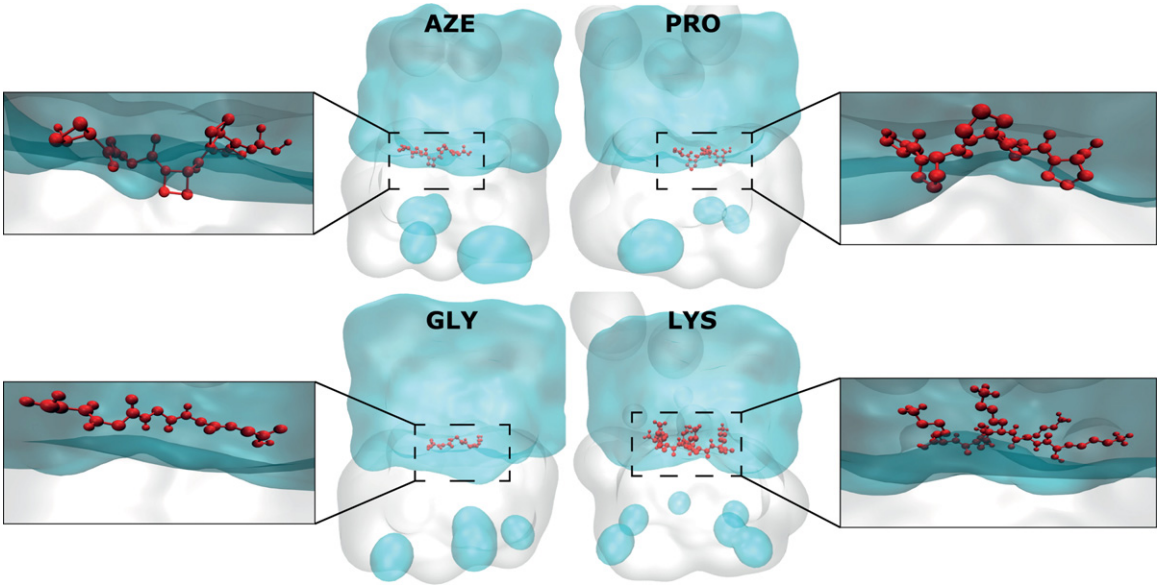


**Fig. 4.** Positioning of the simulated AZE, PRO, GLY, and LYS homo-pentapeptides at 20 ns in bi-phasic systems. The cyan-colour surface refers to water, and the grey surface to non-polar cyclohexane. The homo-pentapeptides are shown in red.

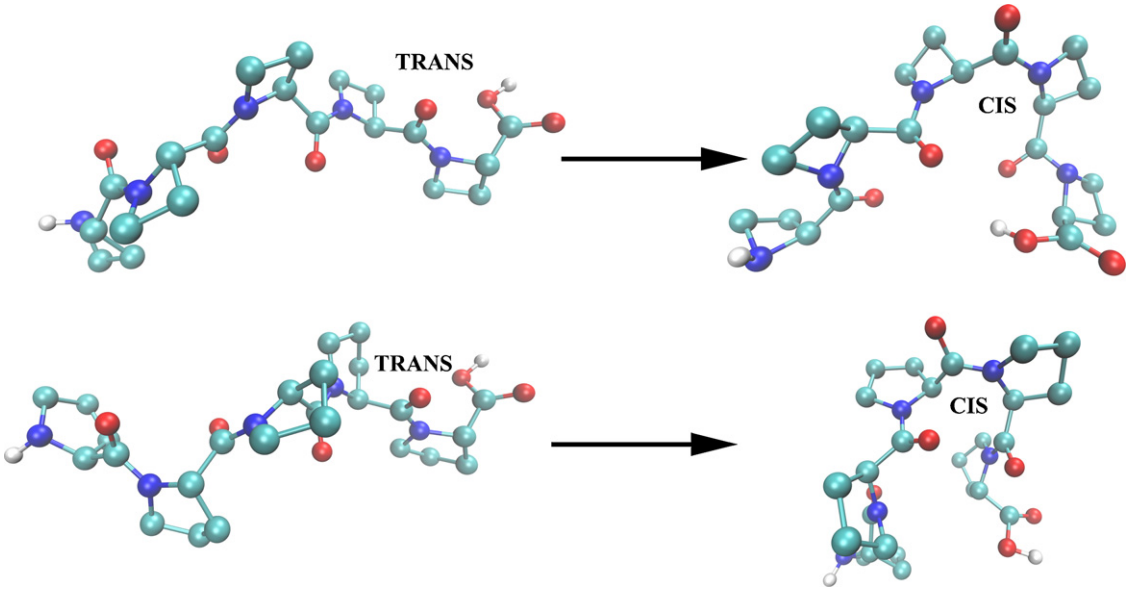


**Fig. 7.** Significant structural effects of the *trans*→*cis* isomerization in Aze and Pro homo-pentapeptides extracted from a 20-ns simulation at 800 °C. The Aze homo-pentapeptide is shown on top, and the Pro homo-pentapeptide is shown at the bottom. The *trans* and *cis* $\omega$ angles are highlighted accordingly.

contexts. As expected, the [CIS] state was seen to be significantly shorter in duration compared to the [TRANS] state in all of the simulations (Fig. 6) that resulted in significantly lower $p_{cis}$ values compared to $p_{trans}$. Interestingly, the *cis* peptide bond conformation on average persisted for 16 to 9 ns longer in the Aze-containing compared to the Pro-containing pepta-peptide. The difference was less pronounced in the case of $\omega_2$ to $\omega_3$, probably due to reduced mobility and stabilization effects of the adjacent flanking residues. The [TRANS] state was also of shorter duration in all Aze- compared to Pro-containing homo-pentapeptides.

Importantly, we were able to confirm that *trans*→*cis* isomerization induces dramatic structural changes in a polypeptide backbone, producing overall more compact structures both in the Aze and Pro homo-pentapeptides simulated here, witnessed throughout the 20-ns trajectory (Fig. 7). Since, to our knowledge, it is not yet known to what extent *cis* peptide bonds conferred by Aze residues can be reversed by prolyl isomerases [68–70,73], these structural implications are of significant importance for the *in vivo* context. Further investigations involving prolyl isomerases and Aze-containing polypeptides would provide invaluable insight into the mechanism of Aze toxicity.

From a biological point of view, the Pro-to-Aze substitution could be predicted to have significant structural effects, as illustrated by previous experimental and modelling studies of Aze-containing peptides, which indicate a preference for *cis* isomerization and formation of gamma turns [74–81]. In extreme cases, increased *trans*→*cis* isomerization resulting from the misincorporation of Aze or related proline derivatives into a polypeptide chain could potentially lead to the formation of a right-handed polyproline type I (PPI) conformation [36,74–78,80–86]. Overall, our results here confirm that Aze more readily favours the *cis* conformation compared to Pro. In addition, it was found that terminal residues in both peptides are more prone to *cis* isomerization compared to the central ones (data not shown). The greater isomerization potential of Aze shown here could be explained in various ways. First, the structural strain caused by the 4-membered ring induces a greater torsion potential on the peptide bond, supported by potential energy measurements being higher in Aze. Second, the smaller ring of the Aze compared to Pro allows for less structural hindrance, allowing for greater flexibility of rotation around the peptide bond.

Previously, we have used the GROMACS software package to study the conformational dynamics of segments of MBP in solution and in association with phospholipid membranes *in silico* [55]. We are now able to use this powerful software package as an additional tool to assess the effects of Pro-to-Aze substitution on MBP and its potential role in demyelinating diseases.

## 4. Concluding remarks

The present study describes in detail the parameterization protocol for Aze in the gromos56a3 force-field implemented in GROMACS. The Aze topology derived here was validated using QM calculations, and computationally evaluated in bi-phasic cyclohexane/water systems against reference amino acids such as Pro, Gly, and Lys. Solvent interaction potential, overall degree of compaction, and *cis*→*trans* and *trans*→*cis* isomerization propensity were all investigated to understand Aze and Pro better in the context of protein structural implications and hydrophobicity. We found a statistically significant 2-fold greater propensity of Aze to adopt a *cis*-peptide bond conformation compared to Pro, both if considering $\omega_1$ to $\omega_4$, and $\omega_2$ to $\omega_3$, within a homo-pentapeptide. The strong isomerization propensity of Aze potentially has significant biological implications. In addition, the *cis* peptide conformation was found to produce conformational changes characterized by more compact overall peptide structures that might influence protein–protein interactions. Clearly, Pro-to-Aze substitutions in the proline-rich region of MBP would affect its conformation and interactions with other molecules with central nervous system myelin. It is essential to understand myelin architecture to decipher the onset and pathogenesis of MS, particularly the early cellular events, and to do so we must determine how the key basic protein of the myelin sheath interacts with membranes and other proteins at the molecular level, to form and stabilize healthy myelin. The modified gromos53a6 will allow researchers to simulate myelin protein systems containing Aze, and to investigate various hypotheses on early events that may lead to multiple sclerosis.

## Acknowledgements

These investigations were made possible by the facilities of the Shared Hierarchical Academic Research Computing Network

(SHARCNET: www.sharcnet.ca) and Compute/Calcul Canada. This work was supported by the Natural Sciences and Engineering Research Council of Canada (Discovery Grant RG121541 to GH). GH is a Tier 1 Canada Research Chair. KAV is the recipient of a Postdoctoral Fellowship from the Multiple Sclerosis Society of Canada. The authors are grateful to Dr. Vladimir Bamm and Dr. Bruno Tomberli (Guelph, Canada) for helpful discussions, and to Mr. Bill Teesdale for software and hardware support.

## Appendix A. Supplementary data

Supplementary data associated with this article can be found, in the online version, at http://dx.doi.org/10.1016/j.jmgm.2012.11.006.

## References

[1] H.M. Berman, E.L. McGandy, J.W. Burgner, R.L. VanEtten, The crystal and molecular structure of L-azetidine-2-carboxylic acid, a naturally occurring homolog of proline, Journal of the American Chemical Society 91 (1969) 6177–6182.
[2] F. Couty, G. Evano, Azetidine-2-carboxylic acid from lily of the valley to key pharmaceuticals: a jubilee review, Organic Preparations and Procedures International 38 (2006) 427–466.
[3] L. Fowden, Azetidine-2-carboxylic acid: a new cyclic imino acid occurring in plants, Biochemical Journal 64 (1956) 323–332.
[4] L. Fowden, Amino acid complement of plants, Phytochemistry 11 (1972) 2271–2276.
[5] L. Fowden, P.J. Lea, E.A. Bell, The nonprotein amino acids of plants, Advances in Enzymology and Related Areas of Molecular Biology 50 (1979) 117–175.
[6] L. Fowden, Non-protein amino-acids of plants, Food Chemistry 6 (1981) 201–211.
[7] L. Fowden, Non-protein acids of plants, Food Chemistry 6 (1981) 201–211.
[8] E. Rubenstein, H. Zhou, K.M. Krasinska, A. Chien, C.H. Becker, Azetidine-2-carboxylic acid in garden beets (*Beta vulgaris*), Phytochemistry 67 (2006) 898–903.
[9] E.A. Bell, Nonprotein amino acids of plants: significance in medicine nutrition, and agriculture, Journal of Agricultural and Food Chemistry 51 (2003) 2854–2865.
[10] L. Fowden, The chemistry and metabolism of recently isolated amino acids, Annual Review of Biochemistry 33 (1964) 173–204.
[11] L. Fowden, M.H. Richmond, Replacement of proline by azetidine-2-carbolic acid during biosynthesis of protein, Biochimica et Biophysica Acta 71 (1963) 459.
[12] B.J. Baum, R.F. Troxler, H.M. Kagan, J.A. Grasso, B. Faris, C. Franzblau, Incorporation of L-azetidine-2-carboxylic acid into hemoglobin in rabbit reticulocytes, Biochemical and Biophysical Research Communications 53 (1973) 1350–1356.
[13] B.J. Baum, L.S. Johnson, C. Franzblau, R.F. Troxler, Incorporation of L-azetidine-2-carboxylic acid into hemoglobin in rabbit reticulocytes *in vitro*, Journal of Biological Chemistry 250 (1975) 1464–1471.
[14] C.S. Trasko, C. Franzblau, R.F. Troxler, Incorporation of L-azetidine-2-carboxylic acid into hemoglobin S in sickle erythrocytes *in vitro*, Biochimica et Biophysica Acta 447 (1976) 425–435.
[15] E.M. Tan, L. Ryhanen, J. Uitto, Proline analogues inhibit human skin fibroblast growth and collagen production in culture, Journal of Investigative Dermatology 80 (1983) 261–267.
[16] T.W. Schwartz, Effect of amino acid analogs on the processing of the pancreatic polypeptide precursor in primary cell cultures, Journal of Biological Chemistry 263 (1988) 11504–11510.
[17] E. Rubenstein, T. McLaughlin, R.C. Winant, A. Sanchez, M. Eckart, K.M. Krasinska, A. Chien, Azetidine-2-carboxylic acid in the food chain, Phytochemistry 70 (2009) 100–104.
[18] P.H. Cameron, E. Chevet, O. Pluquet, D.Y. Thomas, J.J. Bergeron, Calnexin phosphorylation attenuates the release of partially misfolded alpha1-antitrypsin to the secretory pathway, Journal of Biological Chemistry 284 (2009) 34570–34579.
[19] W.F. Prouty, M.J. Karnovsky, A.L. Goldberg, Degradation of abnormal proteins in *Escherichia coli*. Formation of protein inclusions in cells exposed to amino acid analogs, Journal of Biological Chemistry 250 (1975) 1112–1122.
[20] M.M. Grant, A.S. Brown, L.M. Corwin, R.F. Troxler, C. Franzblau, Effect of L-azetidine 2-carboxylic acid on growth and proline metabolism in *Escherichia coli*, Biochimica et Biophysica Acta 404 (1975) 180–187.
[21] N. Verbruggen, M.M. van, E. Messens, Synthesis of the proline analogue [2,3-3H]azetidine-2-carboxylic acid. Uptake and incorporation in *Arabidopsis thaliana* and *Escherichia coli*, FEBS Letters 308 (1992) 261–263.
[22] K. Bessonov, V.V. Bamm, G. Harauz, Misincorporation of the proline homologue Aze (azetidine-2-carboxylic acid) into recombinant myelin basic protein, Phytochemistry 71 (2010) 502–507.
[23] M. Shichiri, C. Hoshikawa, S. Nakamori, H. Takagi, A novel acetyltransferase found in *Saccharomyces cerevisiae* Sigma1278b that detoxifies a proline analogue azetidine-2-carboxylic acid, Journal of Biological Chemistry 276 (2001) 41998–42002.
[24] M. Nomura, S. Nakamori, H. Takagi, Characterization of novel acetyltransferases found in budding and fission yeasts that detoxify a proline analogue azetidine-2-carboxylic acid, Journal of Biochemistry 133 (2003) 67–74.
[25] M. Wada, K. Okabe, M. Kataoka, S. Shimizu, A. Yokota, H. Takagi, Distribution of L-azetidine-2-carboxylate *N*-acetyltransferase in yeast, Bioscience, Biotechnology, and Biochemistry 72 (2008) 582–586.
[26] Y. Lee, R.T. Nagao, C.Y. Lin, J.L. Key, Induction and regulation of heat-shock gene expression by an amino acid analog in soybean seedlings, Plant Physiology 110 (1996) 241–248.
[27] J. Van Rijn, F.A. Wiegant, J. Van den Berg, R. Van Wijk, Heat shock response by cells treated with azetidine-2-carboxylic acid, International Journal of Hyperthermia 16 (2000) 305–318.
[28] E.W. Trotter, C.M. Kao, L. Berenfeld, D. Botstein, G.A. Petsko, J.V. Gray, Misfolded proteins are competent to mediate a subset of the responses to heat shock in *Saccharomyces cerevisiae*, Journal of Biological Chemistry 277 (2002) 44817–44825.
[29] J.C. Guan, C.H. Yeh, Y.P. Lin, Y.T. Ke, M.T. Chen, J.W. You, Y.H. Liu, C.A. Lu, S.J. Wu, C.Y. Lin, A 9 bp *cis*-element in the promoters of class I small heat shock protein genes on chromosome 3 in rice mediates L-azetidine-2-carboxylic acid and heat shock responses, Journal of Experimental Botany 61 (2010) 4249–4261.
[30] K. Dasuri, P.J. Ebenezer, R.M. Uranga, E. Gavilan, L. Zhang, S.O. Fernandez-Kim, A.J. Bruce-Keller, J.N. Keller, Amino acid analog toxicity in primary rat neuronal and astrocyte cultures: implications for protein misfolding and TDP-43 regulation, Journal of Neuroscience Research 89 (2011) 1471–1477.
[31] E. Rubenstein, Biologic effects of and clinical disorders caused by nonprotein amino acids, Medicine 79 (2000) 80–89.
[32] G.A. Chalmers, Swayback (enzootic ataxia) in Alberta lambs, Canadian Journal of Comparative Medicine 38 (1974) 111–117.
[33] I.Y. Adamson, G.M. King, L-azetidine-2-carboxylic acid retards lung growth and surfactant synthesis in fetal rats, Laboratory Investigation 57 (1987) 439–445.
[34] K. Norrby, A. Jakobsson, C.L. Nilsson, Two potentially angiostatic factors a steroid and L-azetidine-2-carboxylic acid, antagonize one another, International Journal of Microcirculation: Clinical and Experimental 13 (1993) 113–124.
[35] K. Norrby, The proline analog L-azetidine-2-carboxylic acid modifies the neovascularization pattern by inhibiting branching or tortuosity and stimulating spatial expansion in the rat mesentery, International Journal of Microcirculation: Clinical and Experimental 12 (1993) 119–129.
[36] E. Rubenstein, Misincorporation of the proline analog azetidine-2-carboxylic acid in the pathogenesis of multiple sclerosis: a hypothesis, Journal of Neuropathology and Experimental Neurology 67 (2008) 1035–1040.
[37] R.A. Sobel, A novel unifying hypothesis of multiple sclerosis, Journal of Neuropathology and Experimental Neurology 67 (2008) 1032–1034.
[38] C.A. Beck, L.M. Metz, L.W. Svenson, S.B. Patten, Regional variation of multiple sclerosis prevalence in Canada, Multiple Sclerosis 11 (2005) 516–519.
[39] S. Tsutsui, P.K. Stys, Degeneration versus autoimmunity in multiple sclerosis, Annals of Neurology 66 (2009) 711–713.
[40] P.K. Stys, Multiple sclerosis: autoimmune disease or autoimmune reaction? Canadian Journal of Neurological Sciences 37 (2010) S16–S23.
[41] P.K. Stys, The axo-myelinic synapse, Trends in Neurosciences 34 (2011) 393–400.
[42] T.J. Murray, The history of multiple sclerosis: the changing frame of the disease over the centuries, Journal of the Neurological Sciences 277 (Suppl. 1) (2009) S3–S8.
[43] G. Harauz, N. Ishiyama, C.M.D. Hill, I.R. Bates, D.S. Libich, C. Farès, Myelin basic protein – diverse conformational states of an intrinsically unstructured protein and its roles in myelin assembly and multiple sclerosis, Micron 35 (2004) 503–542.
[44] J.M. Boggs, Myelin basic protein: a multifunctional protein, Cellular and Molecular Life Sciences 63 (2006) 1945–1961.
[45] J.M. Boggs, Myelin Basic Protein, Nova Science Publishers, Hauppauge, NY, 2008.
[46] G. Harauz, D.S. Libich, The classic basic protein of myelin – conserved structural motifs and the dynamic molecular barcode involved in membrane adhesion and protein–protein interactions, Current Protein and Peptide Science 10 (2009) 196–215.
[47] G. Harauz, V. Ladizhansky, J.M. Boggs, Structural polymorphism and multifunctionality of myelin basic protein, Biochemistry 48 (2009) 8094–8104.
[48] D.S. Libich, G. Harauz, Backbone dynamics of the 18.5 kDa isoform of myelin basic protein reveals transient α-helices and a calmodulin-binding site, Biophysical Journal 94 (2008) 4847–4866.
[49] V.V. Bamm, M. De Avila, G.S.T. Smith, M.A. Ahmed, G. Harauz, Structured functional domains of myelin basic protein: cross talk between actin polymerization and Ca(2+)-dependent calmodulin interaction, Biophysical Journal 101 (2011) 1248–1256.
[50] G.S.T. Smith, M. De Avila, P.M. Paez, V. Spreuer, M.K. Wills, N. Jones, J.M. Boggs, G. Harauz, Proline substitutions and threonine pseudophosphorylation of the SH3 ligand of 18.5-kDa myelin basic protein decrease its affinity for the Fyn-SH3 domain and alter process development and protein localization in oligodendrocytes, Journal of Neuroscience Research 90 (2012) 28–47.
[51] G.S.T. Smith, L. Homchaudhuri, J.M. Boggs, G. Harauz, Classic 18.5- and 21.5-kDa myelin basic protein isoforms associate with cytoskeletal and SH3-domain proteins in the immortalized N19-oligodendroglial cell line stimulated by phorbol ester and IGF-1, Neurochemical Research 37 (2012) 1277–1295.
[52] E. Polverini, G. Rangaraj, D.S. Libich, J.M. Boggs, G. Harauz, Binding of the proline-rich segment of myelin basic protein to SH3-domains – spectroscopic

microarray, and modelling studies of ligand conformation and effects of post-translational modifications, Biochemistry 47 (2008) 267–282.
[53] L. Homchaudhuri, E. Polverini, W. Gao, G. Harauz, J.M. Boggs, Influence of membrane surface charge and post-translational modifications to myelin basic protein on its ability to tether the Fyn-SH3 domain to a membrane *in vitro*, Biochemistry 48 (2009) 2385–2393.
[54] D.S. Libich, M.A.M. Ahmed, L. Zhong, V.V. Bamm, V. Ladizhansky, G. Harauz, Fuzzy complexes of myelin basic protein – NMR spectroscopic investigations of a polymorphic organizational linker of the central nervous system, Biochemistry and Cell Biology (Special issue on Protein Folding: Principles and Diseases) 88 (2010) 143–155.
[55] E. Polverini, E.P. Coll, D.P. Tieleman, G. Harauz, Conformational choreography of a molecular switch region in myelin basic protein – molecular dynamics shows induced folding and secondary structure type conversion upon threonyl phosphorylation in both aqueous and membrane-associated environments, Biochimica et Biophysica Acta 1808 (2011) 674–683.
[56] M.A.M. Ahmed, A.M. De, E. Polverini, K. Bessonov, V.V. Bamm, G. Harauz, Solution NMR structure and molecular dynamics simulations of murine 18.5-kDa myelin basic protein segment (S72–S107) in association with dodecylphosphocholine micelles, Biochemistry 51 (2012) 7475–7487.
[57] D. Van Der Spoel, E. Lindahl, B. Hess, G. Groenhof, A.E. Mark, H.J. Berendsen, GROMACS: fast flexible, and free, Journal of Computational Chemistry 26 (2005) 1701–1718.
[58] B. Hess, C. Kutzner, D. Van Der Spoel, E. Lindahl, GROMACS 4: algorithms for highly efficient load-balanced, and scalable molecular simulation, Journal of Chemical Theory and Computation 4 (2008) 435–447.
[59] C. Oostenbrink, A. Villa, A.E. Mark, W.F. van Gunsteren, A biomolecular force field based on the free enthalpy of hydration and solvation: the GROMOS force-field parameter sets 53A5 and 53A6, Journal of Computational Chemistry 25 (2004) 1656–1676.
[60] A.W. Schuttelkopf, D.M. van Aalten, PRODRG: a tool for high-throughput crystallography of protein–ligand complexes, Acta Crystallographica. Section D: Biological Crystallography 60 (2004) 1355–1363.
[61] J.A. Lemkul, W.J. Allen, D.R. Bevan, Practical considerations for building GROMOS-compatible small-molecule topologies, Journal of Chemical Information and Modelling 50 (2010) 2221–2235.
[62] W.D. Cornell, P. Cieplak, C.I. Bayly, I.R. Gould, K.M. Merz, D.M. Ferguson, D.C. Spellmeyer, T. Fox, J.W. Caldwell, P.A. Kollman, A second generation force field for the simulation of proteins nucleic acids, and organic molecules, Journal of the American Chemical Society 117 (1995) 5179–5197.
[63] W. Humphrey, A. Dalke, K. Schulten, VMD: visual molecular dynamics, Journal of Molecular Graphics 14 (1996) 33–38.
[64] P. Sarkar, C. Reichman, T. Saleh, R.B. Birge, C.G. Kalodimos, Proline *cis–trans* isomerization controls autoinhibition of a signaling protein, Molecular Cell 25 (2007) 413–426.
[65] C. Rubini, P. Ruzza, M.R. Spaller, G. Siligardi, R. Hussain, D.G. Udugamasooriya, M. Bellanda, S. Mammi, A. Borgogno, A. Calderan, L. Cesaro, A.M. Brunati, A. Donella-Deana, Recognition of lysine-rich peptide ligands by murine cortactin SH3 domain: CD ITC, and NMR studies, Biopolymers 94 (2010) 298–306.
[66] A. Borgogno, P. Ruzza, The impact of either 4-R-hydroxyproline or 4-R-fluoroproline on the conformation and SH3(m-cort) binding of HPK1 proline-rich peptide, Amino Acids 2012, http://dx.doi.org/10.1007/s00726-012-1383-y
[67] O. Tchaicheeyan, Is peptide bond cis/trans isomerization a key stage in the chemo-mechanical cycle of motor proteins, FASEB Journal 18 (2004) 783–789.
[68] K.P. Lu, Y.C. Liou, X.Z. Zhou, Pinning down proline-directed phosphorylation signaling, Trends in Cell Biology 12 (2002) 164–172.
[69] Y.C. Liou, A. Sun, A. Ryo, X.Z. Zhou, Z.X. Yu, H.K. Huang, T. Uchida, R. Bronson, G. Bing, X. Li, T. Hunter, K.P. Lu, Role of the prolyl isomerase Pin1 in protecting against age-dependent neurodegeneration, Nature 424 (2003) 556–561.
[70] Y.C. Liou, X.Z. Zhou, K.P. Lu, Prolyl isomerase Pin1 as a molecular switch to determine the fate of phosphoproteins, Trends in Biochemical Sciences 36 (2011) 501–514.
[71] M.S. Friedrichs, P. Eastman, V. Vaidyanathan, M. Houston, S. Legrand, A.L. Beberg, D.L. Ensign, C.M. Bruns, V.S. Pande, Accelerating molecular dynamic simulation on graphics processing units, Journal of Computational Chemistry 30 (2009) 864–872.
[72] C. Dugave, *cis–trans* Isomerization in Biochemistry, Wiley-VCH GmbH, Weinheim, Germany, 2006.
[73] D. Kern, M. Schutkowski, T. Drakenberg, Rotational barriers of *cis*/*trans* isomerization of proline analogues and their catalysis by cyclophilin, Journal of the American Chemical Society 119 (1997) 8403–8408.
[74] A. Zagari, G. Nemethy, H.A. Scheraga, The effect of the L-azetidine-2-carboxylic acid residue on protein conformation. I. Conformations of the residue and of dipeptides, Biopolymers 30 (1990) 951–959.
[75] A. Zagari, G. Nemethy, H.A. Scheraga, The effect of the L-azetidine-2-carboxylic acid residue on protein conformation. II. Homopolymers and copolymers, Biopolymers 30 (1990) 961–966.
[76] A. Zagari, G. Nemethy, H.A. Scheraga, The effect of the L-azetidine-2-carboxylic acid residue on protein conformation. III. Collagen-like poly(tripeptide)s, Biopolymers 30 (1990) 967–974.
[77] F.H. Tsai, C.G. Overberger, R. Zand, Synthesis and peptide bond orientation in tetrapeptides containing L-azetidine-2-carboxylic acid and L-proline, Biopolymers 30 (1990) 1039–1049.
[78] A. Zagari, K.A. Palmer, K.D. Gibson, G. Nemethy, H.A. Scheraga, The effect of the L-azetidine-2-carboxylic acid residue on protein conformation. IV. Local substitutions in the collagen triple helix, Biopolymers 34 (1994) 51–60.
[79] Y.K. Kang, J.S. Jhon, H.S. Park, Conformational preferences of proline oligopeptides, Journal of Physical Chemistry B 110 (2006) 17645–17655.
[80] J.S. Jhon, Y.K. Kang, Conformational preferences of proline analogues with different ring size, Journal of Physical Chemistry B 111 (2007) 3496–3507.
[81] J.L. Baeza, G. Gerona-Navarro, M.J. Perez de Vega, M.T. Garcia-Lopez, R. Gonzalez-Muniz, M. Martin-Martinez, Azetidine-derived amino acids versus proline derivatives. Alternative trends in reverse turn induction, Journal of Organic Chemistry 73 (2008) 1704–1715.
[82] J.C. Horng, R.T. Raines, Stereoelectronic effects on polyproline conformation, Protein Science 15 (2006) 74–83.
[83] Y.K. Kang, H.S. Park, Conformational preferences of pseudoproline residues, Journal of Physical Chemistry B 111 (2007) 12551–12562.
[84] G. Revilla-Lopez, J.G. Warren, J. Torras, A.I. Jimenez, C. Cativiela, C. Aleman, Effects of ring contraction on the conformational preferences of alpha-substituted proline analogues, Biopolymers 98 (2012) 98–110.
[85] J.L. Baeza, M.A. Bonache, M.T. Garcia-Lopez, R. Gonzalez-Muniz, M. Martin-Martinez, 2-alkyl-2-carboxyazetidines as gamma-turn inducers: incorporation into neurotrophin fragments, Amino Acids 39 (2010) 1299–1307.
[86] T.Y. Zheng, Y.J. Lin, J.C. Horng, Thermodynamic consequences of incorporating 4-substituted proline derivatives into a small helical protein, Biochemistry 49 (2010) 4255–4263.